JP1.28 EXAMINATION OF VIEWING ZENITH ANGLE DEPENDENCE ON CLOUD HEIGHTS DERIVED FROM THERMAL INFRARED SATELLITE OBSERVATIONS

Christopher R. Yost*, J. Kirk Ayers, Rabindra Palikonda, Doug Spangenberg, Sunny Sun-Mack, Yan Chen
Science Systems and Applications, Inc., Hampton, VA

Patrick Minnis
NASA Langley Research Center, Hampton, VA

1. INTRODUCTION

Narrow spectral bands in the thermal infrared (IR) atmospheric window (10-12 μm) are commonly used to derive cloud top heights from passive satellite imagers (Minnis et al., 1998). When the field-of-view (FOV) of a satellite imager, such as the Moderate Resolution Imaging Spectroradiometer (MODIS), is completely cloud-filled, the observed brightness temperature at a particular band T_λ can be matched to a local temperature sounding to estimate the cloud top height. Radiation in the IR window is relatively transparent to atmospheric trace gases, so any atmospheric absorption above high-level clouds is usually negligible.

Deep convective clouds (DCC) and other optically thick ice clouds are usually treated as blackbodies in cloud property retrieval algorithms. Therefore it is assumed that the observed 11.0-micron brightness temperature T_{11} corresponds with the physical cloud top. However, recent research suggests that this is not the case. Sherwood et al. (2004b) found that DCC top heights derived from the eighth Geostationary Operational Environmental Satellite (GOES-8) were consistently at least 1 km below the tops observed by the Cloud Physics Lidar (CPL; McGill et al., 2002) during the Cirrus Regional Study of Tropical Anvils and Cirrus Layers-Florida Area Cirrus Experiment (CRYSTAL-FACE). Sherwood et al. (2004a) offered explanations for this phenomenon and concluded that calibration errors were not the cause.

Smith et al. (2008) analyzed cloud heights from GOES-8 and GOES-10 data at the Atmospheric Radiation Measurement (ARM) Southern Great Plains (SGP) site near Lamont, Oklahoma. They compared cloud tops from the traditional IR technique mentioned above and from a CO_2-slicing technique (Smith et al., 1978) to cloud heights from the Active Remotely-Sensed Cloud Locations (ARSCL) products from the ARM program. ARSCL retrieval algorithms use a combination of Micro-Pulse Lidar (MPL) and Millimeter Cloud Radar (MMCR) measurements to derive various cloud products, including cloud boundaries (Clothiaux et al., 2000). Smith et al. (2008) found that both the IR and CO_2-slicing methods underestimated optically thick ($\tau \geq 6$) high-level cloud tops by 1-2 km. Thus it seems that all emission-based cloud height retrievals will underestimate the true physical cloud top, regardless of the wavelength used for the retrieval.

A study by Minnis et al. (2008) compared Aqua-MODIS cloud tops to those from the Cloud-Aerosol Lidar with Orthogonal Polarization (CALIOP) instrument aboard the Cloud-Aerosol Lidar and Infrared Pathfinder Satellite Observations satellite. The Clouds and the Earth's Radiant Energy System (CERES) cloud property retrieval algorithms (Minnis et al., 1995) were used to derive cloud top heights from the Aqua-MODIS radiances, and it was found that the CERES-MODIS cloud top heights were 1-2 km lower than the corresponding CALIPSO cloud heights. An empirical correction was applied to the CERES-MODIS heights, which effectively eliminated the bias between the two datasets.

In the present study, we more closely examine the effect of the satellite viewing zenith angle on the retrieval of cloud heights with IR-based methods. Throughout the rest of this paper we will refer to cloud heights obtained from IR-based methods as the effective radiating height, or simply the effective height, to distinguish it from the physical cloud top. In practice, the effective radiating height lies somewhat lower than the cloud top. The amount by which effective heights underestimate ice-phase cloud tops is related to the ice water content (IWC) at the top of the cloud (Minnis et al., 2008). High IWC near the cloud top causes more extinction of IR radiation upwelling from the lower, warmer layers of the cloud, while low IWC allows more radiation within the cloud to reach the satellite sensor, resulting in a warmer T_{11}. In theory, the viewing zenith angle (VZA) of the satellite sensor has an effect on the effective height retrieval as well. At large VZA, satellite instruments sense more radiation from the upper, colder layers of clouds than at small VZA. This results in a smaller T_{11} and thus a larger effective cloud height is obtained. The effect should be most pronounced for geometrically thick clouds with low IWC sensed from large viewing angles.

2. DATA AND METHODS

2.1 *Cloud height retrievals*

To study the effects of sensor VZA on the retrieval of cloud heights we analyze collocated, nearly-simultaneous observations from the GOES-11 and

* *Corresponding author address:* Christopher R. Yost
1 Enterprise Parkway, Suite 200, Hampton, VA 23666-5986;
e-mail: Christopher.R.Yost@nasa.gov

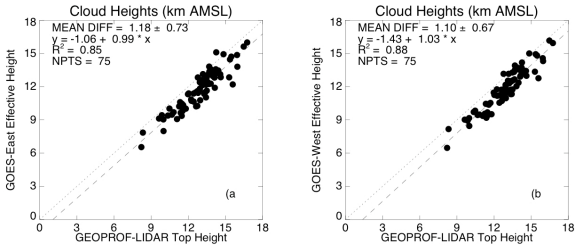

Fig. 1. Comparison of GPL cloud top heights to cloud effective heights from (a) GOES-12 and (b) GOES-11 data.

GOES-12 satellite imagers (Menzel and Purdom, 1994). Both satellites are in geostationary orbit 35,800 km above the equator, with GOES-11 positioned above 135° W longitude and GOES-12 positioned above 75° W longitude. These two satellites provide different views of the central United States where DCC and anvils are ubiquitous, particularly in the summer months. For this study, we analyze a region of the central US extending roughly from 50°N to 20°N and 125°W to 80° W. For daytime FOVs, the 4-channel Visible Infrared Solar-infrared Split-window Technique (VISST) is used to retrieve cloud properties such as thermodynamic phase, optical depth, and effective height, and for nighttime FOVs, the Solar-Infrared Split-window Technique (SIST) is used. Both VISST and SIST match theoretically computed radiances with measured radiances to retrieve cloud properties such as thermodynamic phase, optical depth, and effective height as described by Minnis et al. (1995).

The CALIPSO and CloudSat satellites in the National Aeronautics and Space Administration's (NASA) Afternoon Constellation, or A-Train, provide the opportunity to validate cloud heights from the passive GOES observations with active remote sensors on a larger spatial scale was previously possible with stationary active sensors. CALIPSO carries the CALIOP instrument (Winker et al. 2007), which is sensitive to small cloud and aerosol particles but cannot penetrate optically thick clouds. CloudSat carries a 94-GHz cloud profiling radar (CPR; Mace et al. 2007), which is mainly sensitive to large cloud particles and under most circumstances can penetrate the entire depth of the observed cloud. These two instruments observe our region of interest twice daily between 0800 and 1000 UTC (nighttime) and between 1900 and 2100 UTC (daytime). Here we use the GEOPROF-LIDAR (GPL) dataset, available from Colorado State University, as the "truth" dataset. This product combines cloud information from CALIOP and the CPR into a single dataset. CALIOP provides accurate cloud top information while the CPR is used to filter out multilayer cloud scenarios.

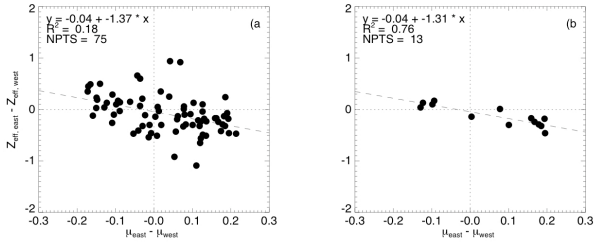

Fig. 2. Difference in cloud effective heights from GOES-12 and GOES-11 as a function of the difference between the cosines of the viewing angles for (a) the same dataset as in Fig. 1 and (b) for cases having a z_{eff} standard deviation less than 150 m.

2.2 *Ice water content retrieval*

As stated by Minnis et al. (2008), there is potential to retrieve IWC estimates near cloud tops with two simultaneous satellite observations from different zenith angles. For remote sensing applications, the IWC of a cloud layer is often expressed as

$$IWC = \frac{2\rho}{3Q}\frac{\mu\tau}{\Delta z}D_e, \tag{1}$$

where the density of ice ρ = 0.9 g cm^{-3}, the visible extinction efficiency Q has a value ~2, τ is the visible optical depth of the cloud layer, μ is the cosine of the satellite zenith angle, Δz is the physical thickness of the cloud layer, and D_e is the effective diameter of the ice particles in the cloud layer. Minnis et al. (2008) showed that τ for the cloud layer between the physical top height of optically thick ice clouds and the retrieved effective height has a value of approximately 1.1. If we have two independent satellite observations with viewing geometry μ_1 and μ_2 then we can define

$$\Delta z_{eff,1} = z_{top} - \Delta z_1, \tag{2}$$

$$\Delta z_{eff,2} = z_{top} - \Delta z_2. \tag{3}$$

Then, taking $\Delta z_{eff,2}$ minus $\Delta z_{eff,1}$ and rearranging gives

$$IWC = 1.1\overline{D}_e \frac{2\rho}{3Q}\frac{\mu_1 - \mu_2}{z_{eff,2} - z_{eff,1}}, \tag{4}$$

where $\overline{D}_e$ is the mean effective particle size from the two observations. This method should provide a reasonable estimate of IWC near the cloud top, which is potentially useful information for determining the risk of aircraft engine icing resulting from large IWC.

3. RESULTS

Figure 1 shows a comparison of the GOES effective heights z_{eff} and the cloud tops from the GPL dataset. The GOES z_{eff} are, on average, approximately 1 km lower than the GPL cloud tops. This result is similar to other studies that compared IR-based satellite cloud height retrievals to cloud heights from active sensors (e.g., Sherwood et al., 2004b; Smith et al., 2008). The mean

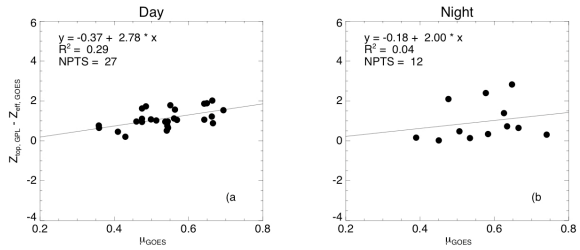

Fig. 3. Difference between GPL cloud top heights and GOES effective heights as a function of GOES μ for (a) daytime and (b) nighttime data.

difference between the GOES-12 (East) and GPL cloud heights (Fig. 1a) is 1.18 km, which is slightly higher than the difference between the GOES-11 (West) and GPL tops (Fig. 1b). This result may be partially explained by the difference in viewing angle between the two satellite instruments, since GOES-12 generally had smaller VZAs than GOES-11 for the cases considered in this study.

Figure 2a shows the difference between the GOES-12 and GOES-11 effective cloud heights as a function of the difference between the cosine of the viewing angles μ. For simplicity in this discussion, we define $\Delta\mu = \mu_{east} - \mu_{west}$, where μ_{east} and μ_{west} are the cosines of the viewing angles from GOES-12 and GOES-11, respectively. Similarly, we define $\Delta z_{eff} = z_{eff,east} - z_{eff,west}$, where $z_{eff,east}$ and $z_{eff,west}$, are the effective heights obtained from the GOES-11 and GOES-12 observations, respectively. As expected $\Delta\mu$ and Δz_{eff} are inversely related. Only data points for which the standard deviation of z_{eff} was less than 150 m are plotted in Figure 2b, resulting in a squared correlation coefficient R^2 of 0.76. As the standard deviation increases, R^2 decreases, stressing the importance of cloud homogeneity. Nevertheless, the inverse relationship between $\Delta\mu$ and Δz_{eff} remains intact even when no z_{eff} standard deviation restriction is imposed, suggesting that the retrieved Δz_{eff} from thermal IR satellite observations tends to approach the true physical cloud top as the sensor viewing angle increases. Given this relationship, it is not surprising that the GOES-12 z_{eff} underestimated the GPL cloud tops slightly more than GOES-11 z_{eff} since the GOES-12 viewing angles were on average approximately 2.3° smaller than the GOES-11 viewing angles. Since three-dimensional cloud effects become more problematic at high viewing angles, it is extremely important that the cloud within the sensor's FOV exhibits little spatial variation.

Figure 3 shows the difference between the GPL cloud tops and the GOES z_{eff} as a function of μ_{goes}. These data were also filtered for clouds exhibiting the most homogeneity. Although there is much scatter, there is a general trend for the difference between the two cloud heights to increase with increasing (decreasing) μ (VZA). The trend is much stronger and has less scatter for the daytime (Fig. 3a) than the nighttime data (Fig. 3b), and it is uncertain why this is

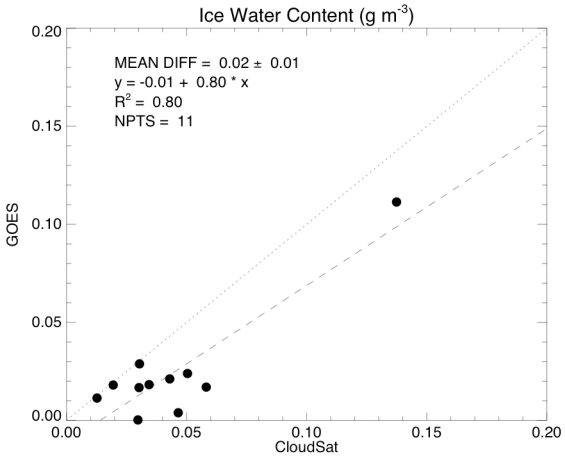

Fig. 4. Comparison of IWC retrievals derived from CloudSat CPR data and simultaneous GOES-11 and GOES-12 data.

the case. While it may be due to greater uncertainty in the cloud optical depths at night, more investigation and data will be required to fully explain this phenomenon.

Figure 4 shows the results of the IWC retrieval from the simultaneous GOES-11 and GOES-12 observations. The GOES values were compared to the radar-derived IWC from the CWC-RO CloudSat product. We compute the cloud-top CWC-RO IWC by taking the mean of the IWC values between z_{top} and z_{eff}. Values below z_{eff} were not considered because it is assumed the satellite sensor cannot detect IR radiation below z_{eff} for an optically thick cloud. Only daytime retrievals of IWC are shown because nighttime particle size retrievals are limited to approximately 50 μm. Furthermore, uncertainties in z_{eff}, can cause the expression $(\mu_1 - \mu_2) / (z_{eff,2} - z_{eff,1})$ in (4) to be negative, which results in unphysical values for IWC. These cases have also been left out of the comparison. For the remaining data, the agreement between the CWC-RO and the GOES retrievals is quite good. The GOES IWC values are generally smaller than the CloudSat values but are on the same order of magnitude as the CloudSat retrievals. Considering the uncertainties associated with matching the two datasets in time and space as well as the uncertainty introduced by slight variations in physical cloud top and particle sizes, these results look fairly promising.

4. DISCUSSION AND CONCLUDING REMARKS

It has been well established in recent research that IR-based retrievals of cloud top height for deep convective and other optically thick ice clouds underestimate the cloud top heights observed by active sensors. The cause is mostly due to relatively small IWC concentrations in the upper portions of the cloud, however it has been shown in the present study that the effect of satellite zenith angle on cloud top height retrievals is quantifiable as well. As the viewing angle

increases, the retrieved effective cloud height approaches the physical cloud height, because at high viewing angles a greater portion of the radiation reaching the sensor comes from the upper, colder portions of the cloud. However, it seems 3-D cloud effects will often complicate the situation. As viewing angle increases, the uncertainties caused by 3-D cloud effects are likely to increase.

Preliminary results of a satellite-based IWC retrieval were shown and compared to values derived by the CPR on the CloudSat satellite. The data were aggressively filtered to find the most homogeneous clouds, and the comparison between the two datasets shows promise. More data and investigation will be necessary to eliminate certain difficulties and fully assess the potential of using simultaneous satellite observations to retrieve cloud-top IWC. Furthermore, it will be necessary to understand the uncertainties in the IWC at cloud top as derived from the CloudSat data. Routine retrieval of cloud-top IWC from satellite observations would be a step forward in assessing aircraft icing risk.

5. REFERENCES

Clothiaux, E. E., T. P. Ackerman, G. G. Mace, K. P. Moran, R. T. Marchand, M. A. Miller, and B. E. Martner, 2000: Objective determination of cloud heights and radar reflectivities using a combination of active remote sensors at the ARM CART sites, *J. Appl. Meteorol.*, 39, 645-665.

Mace, G. G., R. Marchand, Q. Zhang, and G. Stevens, 2007: Global hydrometeor occurrence as observed by CloudSat: Initial observations from summer 2006, *Geophys. Res. Lett.*, 34, L09808, doi:10.1029/2006GL029017.

McGill, M., D. Hlavka, W. Hart, V. S. Scott, J. Spinhirne, and B. Schmid, 2002: Cloud Physics Lidar: Instrument description and initial measurement results, *Appl. Opt.*, 41, 3725-3734.

Menzel, W. P., and J. F. W. Purdom, 1994: Introducing GOES-I: The first of a new generation of Geostationary Operational Environmental Satellites, *Bull. Amer. Meteorol. Soc.*, 75, 757-781.

Minnis, P., et al., 1995: Clouds and the Earth's Radiant Energy System (CERES) algorithm theoretical basis document, volume III: Cloud analyses and radiance inversions (subsystem 4), in *Cloud Optical Property Retrieval (Subsystem 4.3)*, vol. 3, *RP 1376*, 135-176.

Minnis, P., D. P. Garber, D. F. Young, R. F. Arduini, and Y. Takano, 1998: Parameterizations of reflectance and effective emittance for satellite remote sensing of cloud properties, *J. Atmos. Sci.*, 55, 3313-3339.

Minnis, P., C. R. Yost, S. Sun-Mack, and Y. Chen, 2008: Estimating the top altitude of optically thick ice clouds from thermal infrared satellite observations using CALIPSO data, *Geophys. Res. Lett.*, 35, L12801, doi:10.1029/2008GL033947.

Sherwood, S. C., J.-H. Chae, P. Minnis, and M. McGill, 2004a: Underestimation of deep convective cloud tops by thermal imagery, *Geophys. Res. Lett.*, 31, L11102, doi:10.1029/2004GL019699.

Sherwood, S. C., P. Minnis, and M. McGill, 2004b: Deep convective cloud-top heights and their thermodynamic control during CRYSTAL-FACE, *J. Geophys. Res.*, 109, D20119, doi:10.1029/2004JD004811.

Smith, W. L., and C. M. R. Platt: Comparison of satellite-deduced cloud heights with indications from radiosonde and ground-based laser measurements, *J. Appl. Meteorol.*, 17, 1796-1802.

Smith, W. L., Jr., P. Minnis, H. Finney, R. Palikonda, and M. M. Khaiyer, 2008: An evaluation of operational GOES-derived single-layer cloud top heights with ARSCL data over the ARM Southern Great Plains Site, *Geophys. Res. Lett.*, 35, L13820, doi:10.1029/2008GL034275.

Winker, D. M., W. H. Hunt, and M. J. McGill, 2007: Initial performance assessment of CALIOP, *Geophys. Res. Lett.*, 34, L19803, doi:10.1029/2007GL030135.